# Test Structures for Characterising the Fabrication of Miniature Reference Electrodes

# Test Structures for Characterising the Fabrication of Miniature Reference Electrodes

Camelia Dunare[1], Shan Zhang[1], Jamie R. K. Marland[1], Andreas Tsiamis[1], Paul Sullivan[1], Ian Underwood[1], Jonathan G. Terry[1], Anthony J. Walton[1] and Stewart Smith[2]
[1]School of Engineering, Institute for Integrated Micro and Nano Systems,
The University of Edinburgh, Edinburgh, Scotland, UK. Email: Anthony.Walton@ed.ac.uk
[2]School of Engineering, Institute for Bioengineering, The University of Edinburgh,
Edinburgh, Scotland, UK. Email: Stewart.Smith@ed.ac.uk, ORCID: 0000-0002-7004-9219

***Abstract*—Robust and reliable micro-scale integrated electrochemical sensors need a reference electrode that can provide a stable electrochemical potential. This can be achieved using a silver/silver chloride (Ag/AgCl) electrode, produced by the chemical chlorination of a thin patterned silver layer. Well understood and controlled processes are required to produce the Ag/AgCl electrode. This paper shows how previously reported test structures have been used to characterise and inform the fabrication procedure. Wafer mapping of these structures was carried out using a Python controlled measurement system, consisting of a semi-automatic prober connected to an HP4062UX based analyser. The measurements were analysed to determine whether the chlorination process was affected by the test structure geometry. This was found to have no clear effect on chlorination.**

## I. Introduction

Integrated electrochemical sensors are of increasing interest as part of systems for environmental and biomedical sensing applications. One of the most difficult parts of an electrochemical sensor to miniaturise and integrate is the reference electrode which provides a stable and maintainable reference potential. In many applications this can be achieved using a silver/silver chloride (Ag/AgCl) electrode consisting of silver coated with a silver chloride layer. In a microfabricated sensor this can be produced in several ways, but in our implementation, it consists of a patterned thin-film Ag electrode which has been partially converted to AgCl through a chemical chlorination process.

This paper extends the work previously reported at ICMTS 2019 where electrical measurements of bridge resistor test structures were used to measure the conversion of highly conductive silver into AgCl [1]. These previous measurements were all made using a manual prober and so no wafer mapping was performed. It was noted that measurements of the AgCl layers showed a greater than expected variation, indicating that more extensive measurements were required. In the current work, wafer mapping of these structures has been carried out using an automated wafer probing platform.

## II. Test Structure Design and Fabrication

Full detail of the test structures is given in [1]. The wafer layout consists of 16 blocks of 25 identical test chips (Fig. 1A(i)). For the evaluation of the chlorination process the wafer is diced into 16 chips that can be subjected to different processing conditions, each with an array of 5×5 test blocks (Fig. 1A(ii)). Each block contains four-terminal bridge resistance structures with varying dimensions and layouts, as well as Greek cross sheet resistance structures (typically unused) (Fig. 1A(iii),B). This enables various metal layer combinations to be characterised on a single wafer where they are either exposed or protected from the chlorination process. Hence, each process condition results in 25 measurements from each test structure, making wafer mapping possible.

The resistance structures used in this paper were fabricated from a stack of titanium/platinum (bottom, conductor) and titanium/silver (top, test material). They were used to quantify the degree of silver chlorination by assuming conversion of Ag to AgCl, a non-conducting ionic solid compound. Chlorination was performed in 10 mM HCl using solutions of $FeCl_3$ at various concentrations [2].

## III. Electrical Measurement Methods

Measurements were made using a Python controlled measurement system [3], consisting of a semi-automatic prober connected to an HP4062 based analyser, enabling each test structure to be analysed in less than a second. Measurements were performed in "force current, measure voltage" (FIMV) mode, with a 100 μA force current. Simulations suggested that this would create a maximum current density of $10^6$ A $cm^{-2}$ (limiting joule heating to a maximum of 10°C [4]) while providing a measurable voltage drop across the structure under all chlorination conditions (Fig. 2). This was confirmed by measuring a subset of structures at 50 and 100 μA, and the results are presented in Table I. These show no significant increase with current that might be expected if joule heating was present.

Results from Pt-Ag structures shown in Table I indicate that the resistance of the parallel layer of platinum and silver is very close to that of the pure silver structures. As will be shown in the next section, when these structures with Ag exposed to the $FeCl_3$ are fully chlorinated the sheet resistance becomes that of the Pt layer alone.

978-1-6654-8566-1/22/ $31.00 © 2022 IEEE

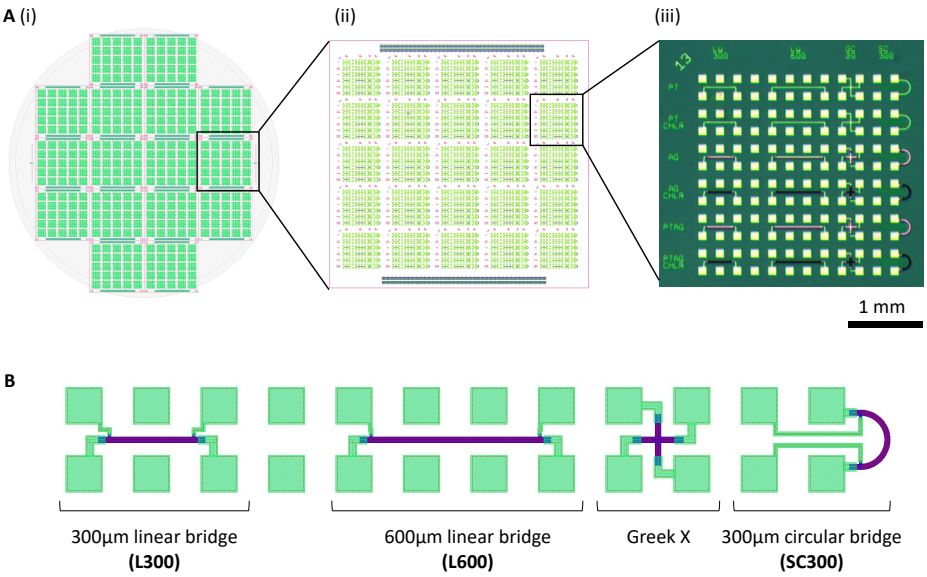


Fig. 1. Test-structure layouts. A: Positions of test-structures at (i) wafer, (ii) die, and (iii) block level. B: Individual test-structures fabricated within each block (Greek cross structures unused in this paper).

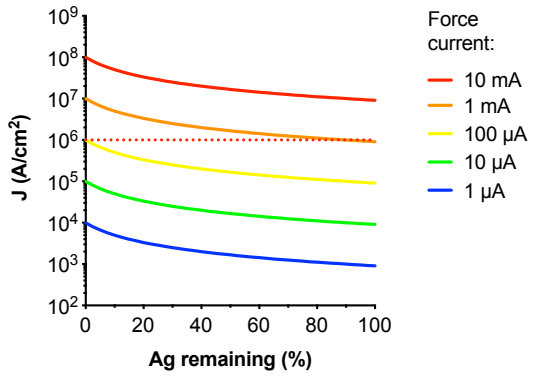


(a)

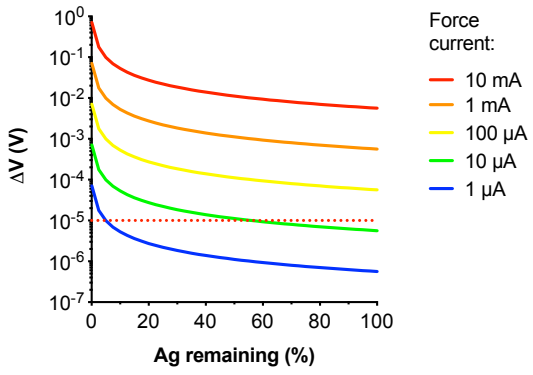


(b)

Fig. 2. Simulated current density/voltage measurements. (a) Simulated current density in AgPt bridge structures, assuming thin-film thicknesses of 50 nm Pt and between 500 nm (100%) and 0 nm (0%) Ag (red dotted line indicates limit of $10^6$ A cm$^{-2}$, above which Joule heating would be significant). (b) Simulated bridge voltages for each forced current (red dotted line indicates limit of $10^{-5}$ V, below which measurement accuracy would be insufficient).

TABLE I
RESULTS FOR PLATINUM AND COMBINED PLATINUM AND SILVER TEST STRUCTURES (LINEAR BRIDGES, $L = 300$ µm), S.D. = STANDARD DEVIATION OF 25 STRUCTURES.

| **Structure** | $I = 50$ µA | | $I = 100$ µA | |
|---|---|---|---|---|
| **Material** | Mean $R$ (Ω) | S.D. | Mean $R$ (Ω) | S.D. |
| Pt | 4.926 | 0.051 | 4.921 | 0.051 |
| Pt-Ag | 0.056 | 0.001 | 0.049 | 0.001 |

## IV. MEASUREMENT RESULTS

### A. *Effects of test structure geometry*

Two nominally identical 300 µm tracks, one straight and one semi-circular (as in a typical reference electrode), along with a 600 µm long straight track, were used to investigate the effect of test-structure geometry using 50 mM $FeCl_3$ and chlorination times of 1 and 10 minutes. The results are shown in figure 3.

These results indicate that complete chlorination is achieved with a 10 minute exposure (bottom row) to the $FeCl_3$ solution, indicated by an increased sheet resistance equivalent to that of the Pt layer. The 1 minute chlorination results (top row) show more variable and incomplete chlorination suggesting that the uniform chlorination model is inadequate and the chemical reaction is not uniform being more rapid at the grain boundaries of the Ag. Control structures of both shapes fabricated only from platinum were unaffected by the chlorination process.

### B. *Effects of processing conditions*

We next investigated how $FeCl_3$ concentration affected chlorination. Test chips were chlorinated for 10 minutes with the following concentrations (mM): 0.25, 0.5, 1, 2, 5, 10 and

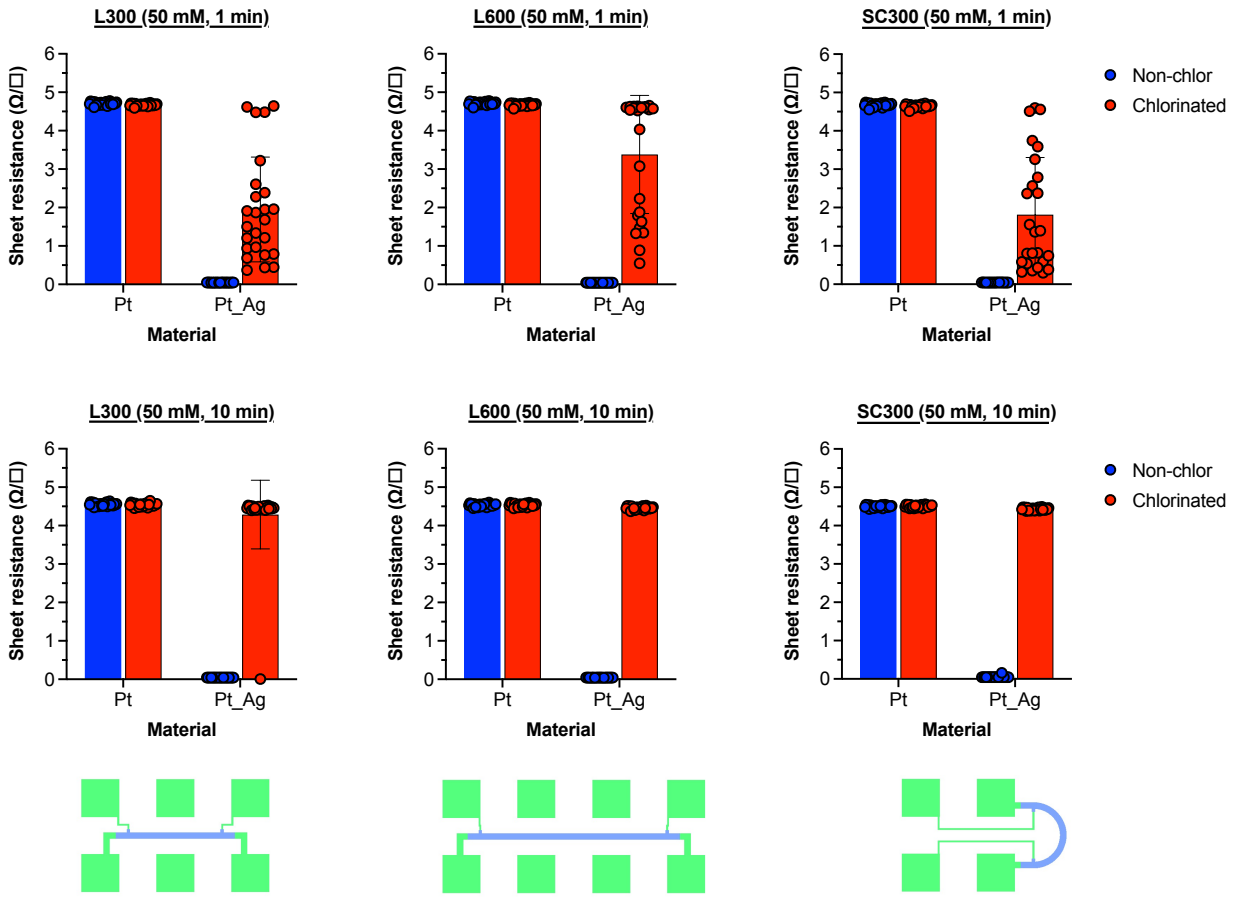


Fig. 3. Results of exposure of three different bridge resistor geometries to 50 mM $FeCl_3$ for 1 minute (top row) and 10 minutes (bottom row).

50. Figure 4 shows the results from exposed Pt-Ag structures along with Pt structures. This allows us to confirm that variation in the sheet resistance of fully chlorinated structures (typically concentrations above 2 mM) is due to variability of the underlying platinum. Figure 5 shows the combined results from the three different geometries for Pt-Ag structures that have been exposed to the chlorination process. These results have been fitted with a sigmoid function. There is no significant difference between the different test structure geometries.

Sheet resistance of both linear and semi-circular test structures showed a dependence on $FeCl_3$ concentration, similar to that observed before [1]. At lower concentrations where there appears to be partial chlorination the results still show that most of the Ag has been converted. For example a measured sheet resistance of 1 Ω/□ indicates that only 3.6% of the silver is remaining. It should be noted that this calculation (and similar calculations of equivalent %ges of remaining Ag reported later) assume uniform conversion. During the chlorination process the conversion to AgCl is more rapid at the grain boundaries and almost certainly transitions though islands of Ag electrically connected via the underlying Pt. The bridge resistor structures provide an averaged value for the sheet resistance.

Optical inspection provided confirmation of these effects (Fig. 6) and showed non-uniformity of chlorination for low concentrations. The automated probe platform enabled substantially more test structures (25 per condition) to be measured than previously, and this showed the variability of resistance of identical structures during the conversion process.

We also observed that chlorination did not proceed uniformly at a microscopic level, with AgCl "patches" forming across the surface of the silver film when low concentrations of $FeCl_3$ were used. We hypothesise that this is due to penetration of the chlorination reagents between grain boundaries in the deposited film (Fig. 7a and 7b) [5]. This non-uniformity would be expected to yield more variable measurements in small structures.

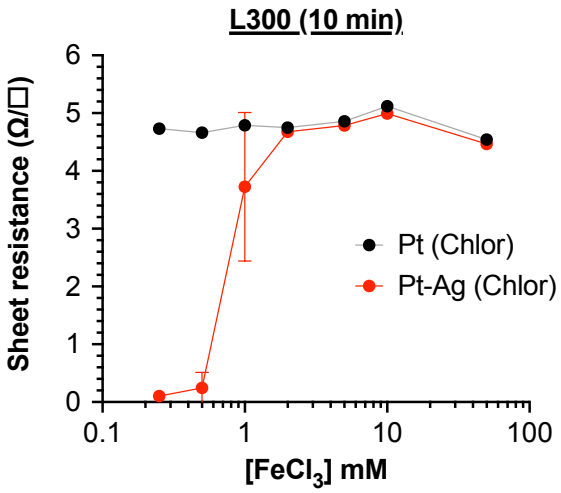


(a) L300 structures chlorinated for 10 minutes

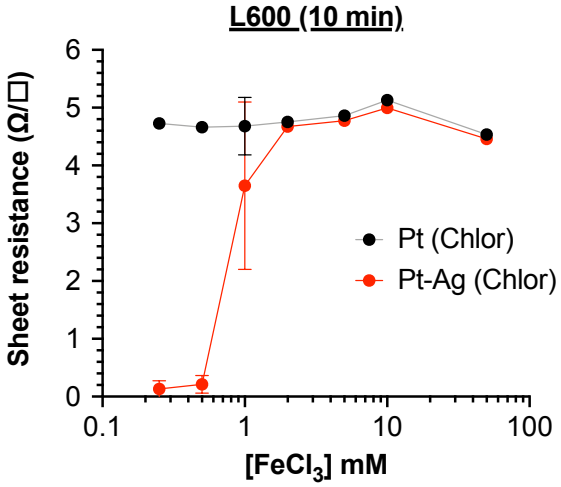


(b) L600 structures chlorinated for 10 minutes

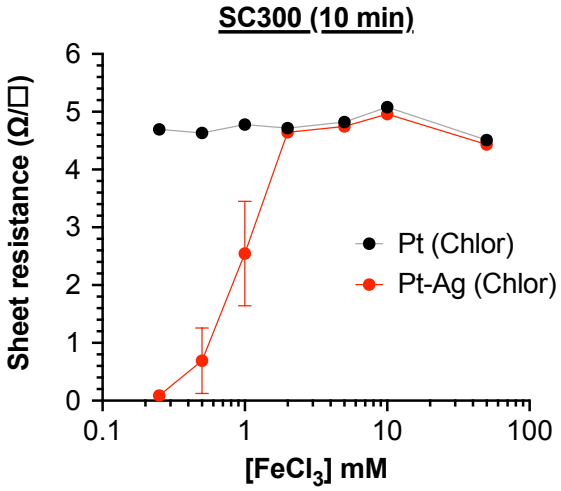


(c) SC300 structures chlorinated for 10 minutes

Fig. 4. Effects of chlorination concentration. Measurements of 25 structures at each chlorination condition. Error bars are standard deviation, $n = 25$.

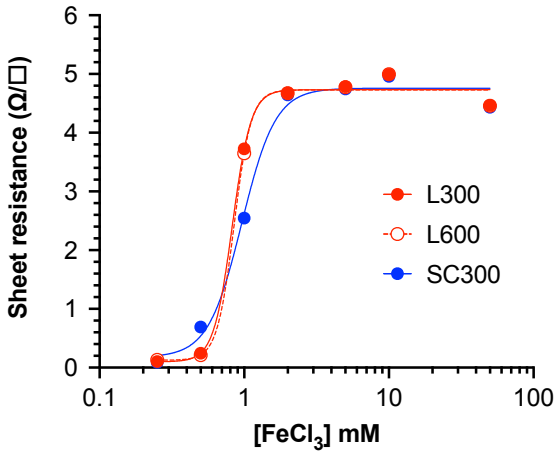


Fig. 5. Combined results from the three different geometries.

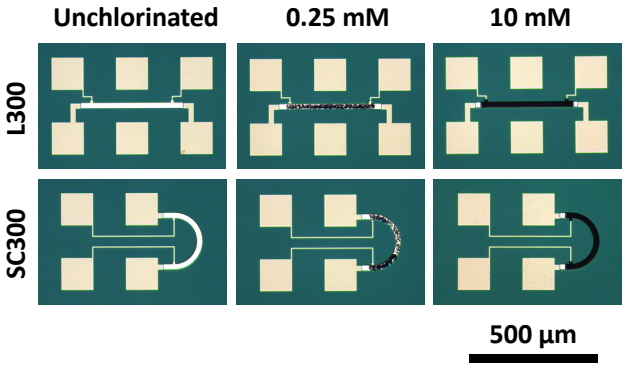


Fig. 6. Optical inspection of test structures

### C. Cross-die and cross wafer mapping of sheet resistance

We conducted die-level mapping of the sheet resistance from chlorinated Pt/Ag and non-chlorinated Pt linear bridge structures (using the array of 5×5 test blocks). This showed a spatial pattern of non-uniformity, with sheet resistance measurements giving larger values in the top-left of the die, and smaller values in the bottom left (Fig. 8). Interestingly the same pattern was evident for both Pt and chlorinated PtAg, suggesting that the underlying Pt was responsible for the variability. As previously stated, the measured sheet resistance of the Pt-Ag structures is a parallel combination of the two layers such that:

$$R_T = \frac{R_{\mathrm{Ag}} R_{\mathrm{Pt}}}{R_{\mathrm{Ag}} + R_{\mathrm{Pt}}} \tag{1}$$

where $R_T$ is the total resistance and $R_{\mathrm{Ag}}$ and $R_{\mathrm{Pt}}$ are the resistances of the silver and platinum layers respectively. We can extract the resistance of the Ag layer alone using the following equations where the value of $R_{\mathrm{Pt}}$ is found from Pt structures adjacent to the chlorinated Pt-Ag structures.

$$R_{\mathrm{Ag}} = \frac{R_T R_{\mathrm{Pt}}}{R_{\mathrm{Pt}} - R_T} \tag{2}$$

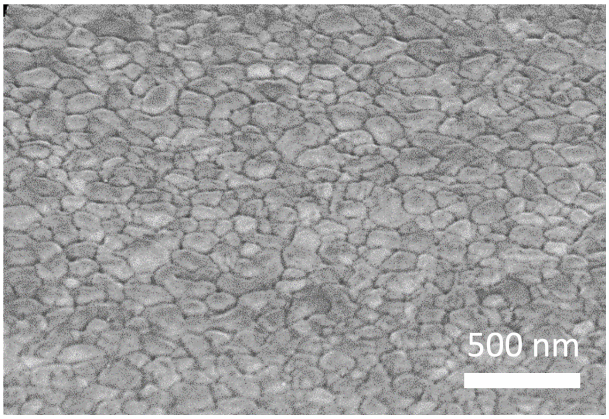


(a)

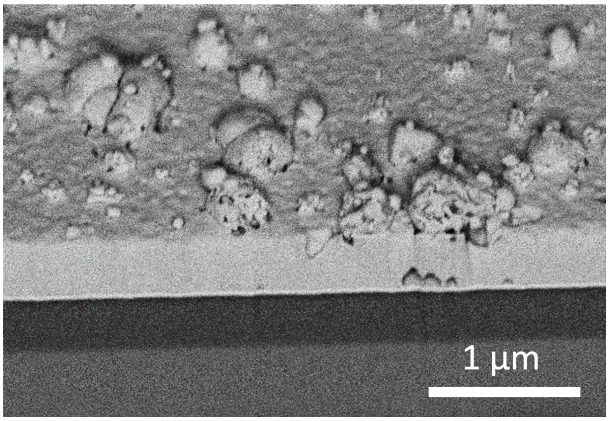


(b)

Fig. 7. Scanning electron microscope images showing (a) thin-film silver deposited using e-beam evaporation, showing grain boundaries, (b) partially chlorinated silver.

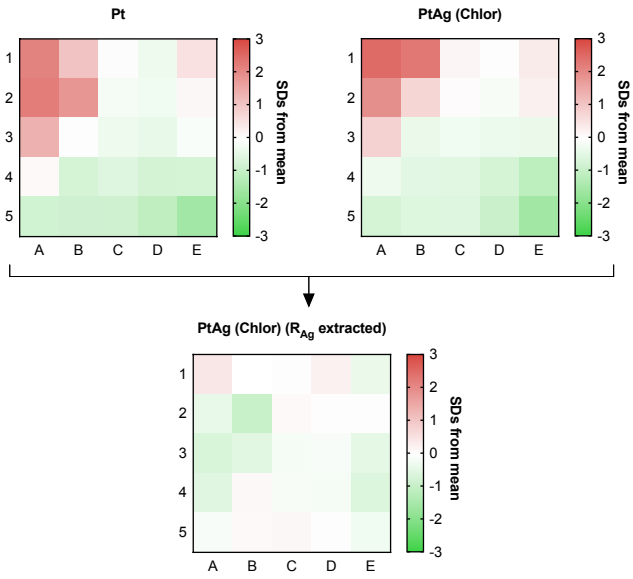


Fig. 8. Cross-die spatial distribution of non-uniformity from 300µm linear bridges following chlorination with 50 mM $FeCl_3$, showing Pt-only structures on the left, PtAg structures on the right and the resulting cross-die spatial distribution of non-uniformity in silver sheet resistance.

Extraction of $R_{\mathrm{Ag}}$ from the total resistance using this technique is also shown in the die map at the bottom of Fig 8. This indicates that "Pt only" control structures are needed for accurate assessment of Pt/Ag chlorination and variability.

Finally, we have performed chlorination of a full wafer of test structures, meaning 16 blocks of 25 test chips as shown in Fig. 1A. This wafer was prepared using the same process as the previous results but due to an unexpected change in the deposition process the Ag thickness was observed to be about 380 nm compared to the 520 nm for the other results. The wafer was chlorinated for 10 minutes with a $FeCl_3$ concentration of 0.5 mM on a shaker table operating at 75 rpm.

Fig.9 shows the results of electrical measurements of 300 µm linear structures. The top row shows results from protected Pt and Pt-Ag structures, while the bottom row shows results from structures exposed to the $FeCl_3$ solution. The left hand and centre columns show the sheet resistance of the Pt and Pt-Ag structures, while the right hand column shows the extracted Ag sheet resistance using the previously described method. White blocks in the wafer maps indicate sheet resistances outside the range of the scale bar.

The chlorinated Ag results (bottom right) show considerable variation for this process condition, which may be due to uneven mixing of the chlorination solution due to the motion of the shaker table. In order to look at this in more detail the Ag sheet resistance (which is an average of the contribution of remaining grains of silver along the length of the structure) has been turned into an estimate of the percentage of Ag remaining, see Fig. 10. This indicates that less than 1% of the silver remains unchlorinated and is contributing to the resistance measurement.

## V. Conclusion

Here we show that resistance test structures, fabricated from a stack of Pt-Ag, can be used to measure conversion of Ag to AgCl during fabrication of miniaturised reference electrodes. An automated prober was used to enable large numbers of structures to be measured and meaningful statistics to be produced. Accurate analysis of the structures was found to require adjacent Pt-only structures to enable extraction of the Ag resistance. Our investigation of AgCl formation revealed a concentration-dependent effect of the oxidant $FeCl_3$. This was confirmed using optical and electron microscopy. No clear effect of structure geometry was evident. Finally, we demonstrated wafer mapping of AgCl formation, indicating that the method is suitable for process monitoring during wafer-level microsensor manufacturing.

## References

[1] C. Dunare et al., "Test Structures for Characterising the Silver Chlorination Process During Integrated Ag/AgCl Reference Electrode Fabrication," *2019 IEEE 32nd International Conference on Microelectronic Test Structures (ICMTS)*, 2019, pp. 58-63, doi: 10.1109/ICMTS.2019.8730966.

[2] B.Beverskog, I.Puigdomenech, "Revised pourbaix diagrams for iron at 25–300 °C", *Corrosion Science*, Volume 38, Issue 12, December 1996, Pages 2121-2135, doi.org/10.1016/S0010-938X(96)00067-4

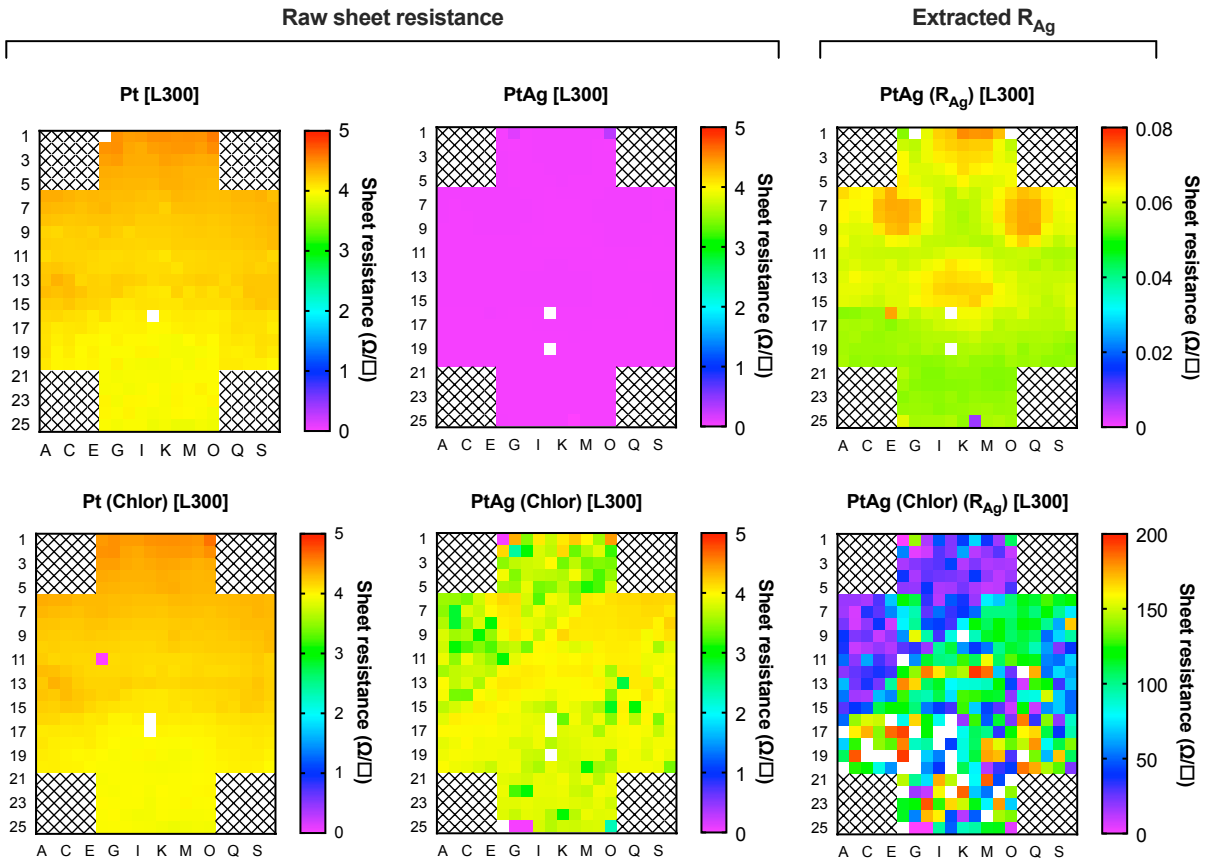


Fig. 9. Full wafer sheet resistance maps.

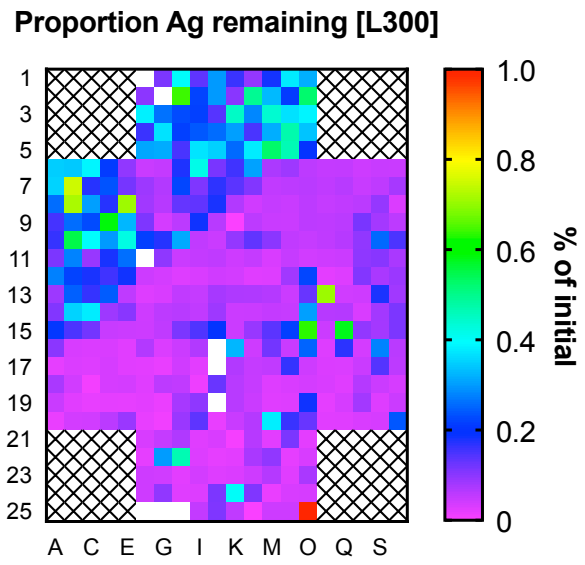


Fig. 10. Full wafer map of chlorinated Pt-Ag results estimating percentage of remaining silver.


[3] P. Sullivan, A. Tsiamis, M. Rondé, A. J. Walton, S. Smith and J. G. Terry, "Automated Generation, Fabrication and Measurement of Parametric Test Structures for Rapid Prototyping Using Optical Maskless Lithography," *2020 IEEE 33rd International Conference on Microelectronic Test Structures (ICMTS)*, 2020, pp. 1-6, doi: 10.1109/ICMTS48187.2020.9107929.

[4] J. R. Back, "Current Limitations of thin Film Conductors," *20th International Reliability Physics Symposium*, 1982, doi: 10.1109/IRPS.1982.361949

[5] H. Ha and J. Payer, "The effect of silver chloride formation on the kinetics of silver dissolution in chloride solution," *Electrochimica Acta*, vol. 56, no. 7, pp. 2781–2791, 2011.